FEBS Letters

FEBS PRESS science publishing by scientists

An experimental comparison of human and bovine rhodopsin provides insight into the molecular basis of retinal disease

James M. Morrow[1,2,*], Gianni M. Castiglione[1], Sarah Z. Dungan[2], Portia L. Tang[1,2], Nihar Bhattacharyya[1], Frances E. Hauser[2] and Belinda S.W. Chang[1,2,3]

1 Department of Cell and Systems Biology, University of Toronto, Canada
2 Department of Ecology and Evolutionary Biology, University of Toronto, Canada
3 Centre for the Analysis of Genome Evolution and Function, University of Toronto, Canada

Correspondence
Belinda S.W. Chang, Department of Cell and Systems Biology, University of Toronto, Toronto M5S 3G5, Canada
Fax: +1 416 978 8532
Tel: +1 416 978 3507
E-mail: belinda.chang@utoronto.ca

***Present address**
Centre of Forensic Sciences, Toronto, Canada

(Received 10 February 2017, revised 22 March 2017, accepted 25 March 2017, available online 31 May 2017)

doi:10.1002/1873-3468.12637

Edited by Peter Brzezinski

Rhodopsin is the visual pigment that mediates dim-light vision in vertebrates and is a model system for the study of retinal disease. The majority of rhodopsin experiments are performed using bovine rhodopsin; however, recent evidence suggests that significant functional differences exist among mammalian rhodopsins. In this study, we identify differences in both thermal decay and light-activated retinal release rates between bovine and human rhodopsin and perform mutagenesis studies to highlight two clusters of substitutions that contribute to these differences. We also demonstrate that the retinitis pigmentosa-associated mutation G51A behaves differently in human rhodopsin compared to bovine rhodopsin and determine that the thermal decay rate of an ancestrally reconstructed mammalian rhodopsin displays an intermediate phenotype compared to the two extant pigments.

Keywords: opsin; retinal disease; retinitis pigmentosa; vision; visual pigment

Rhodopsin is the visual pigment expressed in rod photoreceptors of the retina and is responsible for mediating dim-light vision in vertebrates [1]. Rhodopsin is a heptahelical integral membrane protein that serves as a model system for class A (rhodopsin-like) G protein-coupled receptors (GPCRs), despite the unique interaction it shares with its light-sensitive ligand, 11-*cis*-retinal, to which it is bound through a Schiff base linkage at K296 [2]. Most vertebrate rhodopsin pigments have a wavelength of maximum absorbance (λ_{MAX}) between 490 and 500 nm, with certain groups occasionally falling outside this range [3,4]. Visual transduction begins with photoisomerization of the chromophore to all-*trans*-retinal, which causes a series of conformational changes in rhodopsin, eventually leading to the biologically active metarhodopsin II (meta II) state [5]. Thermal energy can also trigger spontaneous visual pigment activation, leading to dark noise that interferes with light detection by producing a false signaling response [6]. For rhodopsin to regenerate *in vivo*, all-*trans*-retinal must be released to allow new 11-*cis*-retinal to enter the chromophore-binding pocket and form a new Schiff base linkage with opsin, restoring photosensitivity [7].

Retinitis pigmentosa (RP) is a degenerative retinal disorder caused by mutations to components of the visual transduction cascade that leads to symptoms including decreasing visual fields and progressive visual impairment, sometimes even resulting in complete blindness [8]. Mutations in rhodopsin account for

Abbreviations
DM, N-dodecyl-D-maltoside; GPCRs, G protein-coupled receptors; meta II, metarhodopsin II; RP, retinitis pigmentosa; TM, transmembrane helices.

~ 30–40% of all cases of autosomal dominant RP, which can be associated with a wide range of structural motifs, including transmembrane helices (TM) [9], N- and C-termini [10,11], and interhelical loops [12]. *In vitro* studies of rhodopsin structure and function have been essential in helping to identify the functional changes in rhodopsin due to RP-associated mutations [13–15]. These functional abnormalities can include a decreased ability to bind chromophore, an inability to properly fold during translation, and decreased stability of the dark or activated state, and have led to general classifications of RP mutations types based on these molecular phenotypes [16].

Bovine rhodopsin has been the subject of the vast majority of studies of rhodopsin structure and function, including those examining mutations that cause visual disease. This is largely due to the traditionally wide availability of cow eyes, along with the development of protocols to extract rhodopsin directly from retinal tissue [17]. Historically, this placed bovine rhodopsin as the *de facto* representative of not only mammalian rhodopsins but also all class A GPCRs, and this meant that any insights into rhodopsin were typically made in the bovine model. More recently, studies of nonmodel organisms have illustrated that there are significant differences in rhodopsin structure and function among vertebrates [3,18,19], and even within mammalian rhodopsins [20,21]. Despite these differences, bovine rhodopsin remains the primary system used to study human retinal disease caused by changes in rhodopsin function [22].

In order to properly interpret studies of bovine rhodopsin that concern inherited retinopathies most relevant to humans, such as RP, it is important to have a clear understanding of the functional differences between bovine and human rhodopsin. Several aspects of human rhodopsin function have been shown to differ from bovine rhodopsin, such as λ_{MAX} [23,24] and the kinetics of light activation [21,25], suggesting that functional discrepancy exists between the two visual pigments despite minimal sequence variation. Moreover, investigating the trajectory of functional differences between human and bovine rhodopsin can be better understood through examining ancestrally reconstructed mammalian rhodopsins [26], which may shed light on the relationship between rhodopsin function and amino acid variation among present day pigments.

In this study, we highlight differences in λ_{MAX}, dark state thermal decay, and light-activated retinal release between bovine and human rhodopsin. We also perform site-directed mutagenesis in a human rhodopsin background to elucidate the molecular basis of these differences. Furthermore, we engineer a mutation associated with RP, G51A, in human rhodopsin that shows a significantly different effect on function than the same mutation in bovine rhodopsin. Finally, we further characterize the ancestrally reconstructed rhodopsin sequence of the mammalian node in order to better understand the functional evolution of mammalian rhodopsins. This study highlights the potential of comparative *in vitro* studies to provide insight into both the molecular mechanisms of disease phenotypes, and the contribution of sequence diversity to the evolution of protein function.

Materials and methods

Cloning and mutagenesis

The coding sequences of bovine [27] and human [28] rhodopsin were amplified using *Pfu* DNA Polymerase (Fermentas, Waltham, MA, USA) and inserted into the pJET1.2 cloning vector (Fermentas). Site-directed mutagenesis primers were designed to induce amino acid substitutions at seven sites (213, 216, 266, 270, 297, 298, 300), introducing bovine rhodopsin identities into the human rhodopsin sequence; the *retinitis pigmentosa* mutation G51A was also introduced into both bovine and human rhodopsin sequences. Mutagenesis was performed via PCR following the QuikChange site-directed mutagenesis protocol (Agilent, Santa Clara, CA, USA) and using PfuUltra II Fusion HS DNA Polymerase (Agilent). Wild-type and mutant sequences of bovine and human rhodopsin were ligated into the p1D4-hrGFP II expression vector [29]. All plasmid sequences were verified using a 3730 DNA Analyzer (Applied Biosystems, Foster City, CA, USA).

Visual pigment expression and purification

Expression vectors were used to transiently transfect cultured HEK293T cells using Lipofectamine 2000 (Invitrogen, Carlsbad, CA, USA). Cells were harvested 48 h post-transfection and opsins were regenerated in the dark using 11-*cis*-retinal, generously provided by Rosalie Crouch (Medical University of South Carolina). Visual pigments were solubilized in HEPES buffer (50 mM HEPES, 140 mM NaCl, 3 mM $MgCl_2$, pH 7) containing 1% N-dodecyl-D-maltoside (DM) and immunoaffinity purified using the 1D4 monoclonal antibody [30] covalently coupled to UltraLink Hydrazide resin (Thermo Scientific, Waltham, MA, USA). Purified visual pigment samples were eluted in sodium phosphate buffer (50 mM NaPhos, 0.1% DM, pH 7).

Absorbance spectroscopy

The ultraviolet-visible absorption spectra of rhodopsins were recorded at 25 °C using a Cary 4000 double-beam spectrophotometer (Agilent). All λ_{MAX} values were calculated after fitting absorbance spectra to a standard template for A1

visual pigments [31]. A shift in λ_{MAX} to ~ 380 nm was observed following a 30-s light bleach with a fiber optic lamp (Dolan-Jenner, Boxborough, MA, USA), representing the biologically active meta II intermediate. Thermal decay was monitored as the decrease in absorbance at λ_{MAX} while incubating at 45 °C in the dark. Spectra of rhodopsin samples (1.2–2.0 μM) were recorded every 20 min and temperature was maintained by a Peltier-based temperature controller (Agilent). Mineral oil was used to prevent evaporation due to a long incubation at high temperature and a high scan rate (2000 nm·min^{-1}) prevented any detectable photoactivation. Absorbance data were converted to natural logarithms and plotted against time. A linear regression ($y = a + bx$) was fit to the data, while half-life values were calculated based on the slope 'b' ($t_{1/2} = \ln 2/b$). All linear regressions used to calculate half-life values resulted in r^2 values > 0.95.

Fluorescence spectroscopy

Retinal release following rhodopsin light-activation was monitored using a Cary Eclipse fluorescence spectrophotometer equipped with a Xenon flash lamp (Agilent), based on a protocol originally established in a previous study [32], with modifications and specific parameters being previously noted [19]. Briefly, 0.1–0.2 μM rhodopsin samples were bleached for 30 s at 20 °C with a fiber optic lamp (Dolan-Jenner), while collecting fluorescence measurements at 30-s intervals. Data were fit to a three-variable, first-order exponential equation ($y = y_o + a(1-e^{-bx})$), with half-life values calculated based on the rate constant 'b' ($t_{1/2} = \ln 2/b$). All curve fitting resulted in r^2 values of > 0.95.

Statistical analyses

To evaluate whether the effect of G51A on retinal release was significantly different between the bovine and human backgrounds, we used a two-way analysis of variance (ANOVA) [33]. To test for an interaction effect between the species background and the G51A mutation, we set up the analysis to have the residue at site 51 as the first factor and species as the second factor (e.g. [34]). As such, comparisons between human and bovine rhodopsin were made in the wild-type backgrounds, and G51A mutants for each species. Both factors had nonsignificant ($P > 0.05$) differences in variance (Levene's tests) and residuals were normally distributed. To correct for multiple tests, *post hoc* pairwise comparisons between ANOVA groups were assessed using Tukey's statistic [35].

Results

Kinetic rates of human rhodopsin differ from bovine rhodopsin

Purified human and bovine rhodopsin both formed Schiff base linkages with 11-*cis*-retinal, producing dark spectra with λ_{MAX} values of 494.0 ± 0.12 nm and 498.5 ± 0.06 nm, respectively (Fig. 1A,B), which is consistent with previously established values [23,24]. Following a light bleach of 30 s, λ_{MAX} values shift to ~ 380 nm, characteristic of the biologically active meta II intermediate, indicating both rhodopsins properly activate in response to light (Fig. 1A,B inset). The thermal decay of the dark state was evaluated by incubating rhodopsin in the dark at 45 °C and monitoring the decrease in absorbance at λ_{MAX} over time (Fig. 1C,D), which has been associated with isomerization of the chromophore and hydrolysis of the Schiff base linkage [14,36]. Interestingly, the half-life of thermal decay for human rhodopsin was three times longer ($t_{1/2}$ = 445.5 ± 10.55 min; rel-$t_{1/2}$ = 3.00) than that of bovine rhodopsin ($t_{1/2}$ = 148.7 ± 2.78 min; rel-$t_{1/2}$ = 1.00; Fig. 1E,F). Additionally, in order to investigate the stability of the meta II intermediate, a fluorescence assay was used to monitor the rate of release of all-*trans*-retinal following photoactivation at 20 °C. The half-life of retinal release for bovine rhodopsin was 15.5 ± 0.35 min, similar to previously recorded values [19,37], while that of human rhodopsin was significantly shorter at 11.8 ± 0.38 min (Fig. 1G). Retinal release half-lives were also recorded at two additional temperatures (16 °C, 25 °C) in order to construct Arrhenius plots to compare activation energies of light-activated Schiff base hydrolysis (Table 1). Despite human rhodopsin having shorter half-life values at each temperature point, activation energies of both human (21.6 ± 1.3 kcal) and bovine rhodopsin (21.3 ± 1.7 kcal) remained nearly identical (Fig. 1H). These values are also similar to literature values of several rhodopsins [19] and a cone opsin [38]. These results highlight that significant differences in both dark and activated state kinetic functions exist between these two mammalian rhodopsins, which were further investigated with mutagenesis experiments.

Sites 297 and 298 are functional determinants of bovine and human rhodopsin

Substitutions were made in human rhodopsin at sites 297, 298, and 300, changing them to bovine rhodopsin amino acid identities (S297T, A298S, I300V) to investigate the contributions of these sites to the functional differences between human and bovine rhodopsins. While S297T (495.2 nm) and A298S (495.7 nm) caused redshifts in λ_{MAX} compared to wild-type, the shift produced by I300V (494.8 nm) was smaller, less than a nanometer from wild-type (Fig. 2A). The relative half-life of thermal decay of S297T was almost identical to bovine rhodopsin (1.10), causing a larger shift than

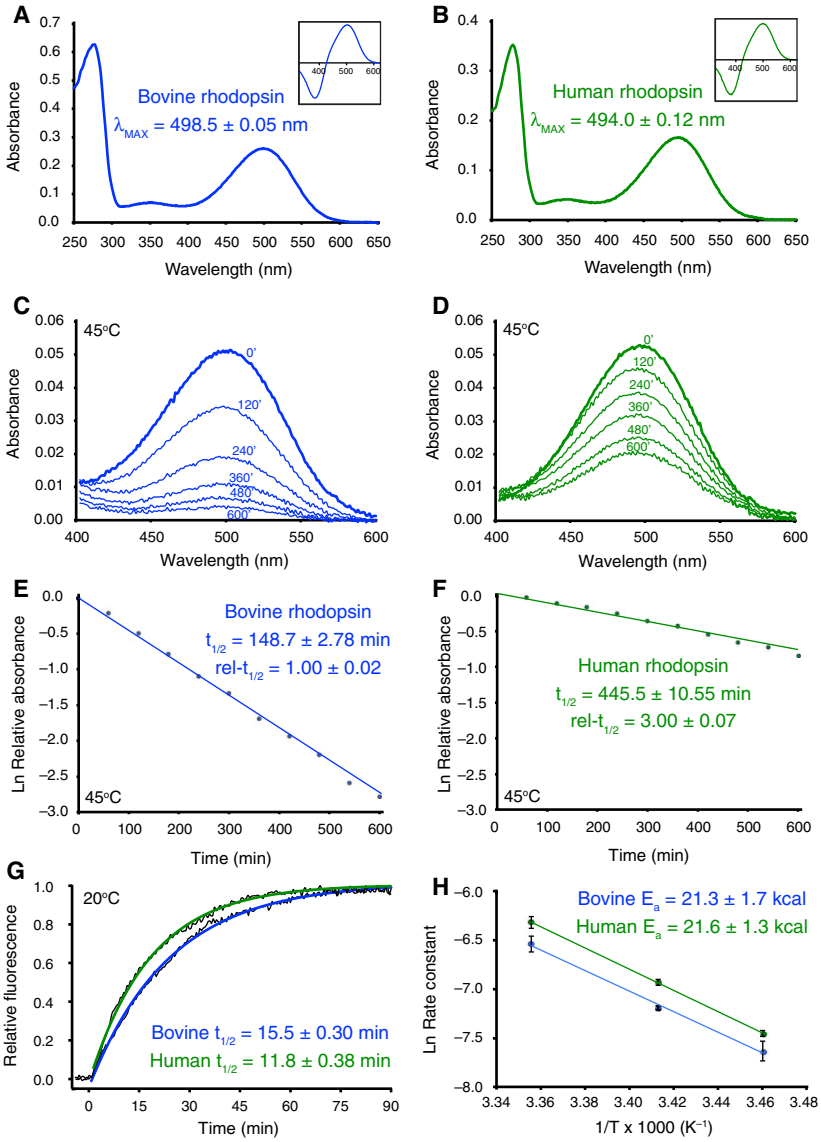

Fig. 1. Comparative analysis of *in vitro* function between bovine and human rhodopsin. Dark spectra of (A) bovine rhodopsin and (B) human rhodopsin, used to estimate λ_{MAX} values by curve fitting to A1 visual pigment templates. Respective difference spectra (inset) were produced by subtracting activated spectra following a 30-s light bleach, resulting in a complete conversion into meta II, from dark spectra. Incubating (C) bovine rhodopsin and (D) human rhodopsin at 45 °C in the dark led to a decrease in absorbance, which can be plotted against time (E–F) to determine the rate of thermal decay. Increase in fluorescence due to release of all-*trans*-retinal following photoactivation (G) in bovine and human rhodopsin, with half-life values calculated based on the resulting first-order kinetic reactions. An Arrhenius plot (H) of the natural logarithm of retinal release rates at a variety of temperatures is used to estimate activation energies (E_a) based on the negative reciprocal of the slope of a linear regression line that best fit the data.

either A298S (1.77) or I300V (2.22; Fig. 2B). Shifts in light-activated retinal release rates were also varied among these three substitutions, with S297T (14.3 ± 0.23 min) again shifting function closer to bovine rhodopsin, while A298S (21.1 ± 1.11 min) resulted in a much slower rate, and I300V (9.9 ± 0.15 min) in contrast had an even faster rate than wild-type human rhodopsin (Fig. 2C). The influence of these substitutions may act directly with the Schiff base and/or indirectly with the nearby N55-D83-N302 hydrogen-bonding network (Fig. 2D). When all three mutations were combined, the resulting functional shifts were of smaller magnitude than the more extreme

Table 1. Light-activated retinal release values measured at various temperatures used to construct an Arrhenius plot.

Visual pigment	Temperature (°C)	Light-activated retinal release half-life (min)[a]
Bovine rhodopsin	16	24.0 ± 2.44 (3)
	20	15.5 ± 0.30 (16)
	25	8.1 ± 0.60 (7)
Human rhodopsin	16	19.9 ± 0.50 (3)
	20	11.8 ± 0.39 (8)
	25	6.4 ± 0.41 (3)

[a] Values reported as mean ± standard error and number of replicates in parentheses.

effects seen for each property by single mutations (Fig. 2E; Table 2). These results imply that sites 297 and 298 likely play a larger role in mediating rhodopsin function than site 300, while also suggesting that the combination of all three mutations may mitigate more drastic shifts caused by any single substitution.

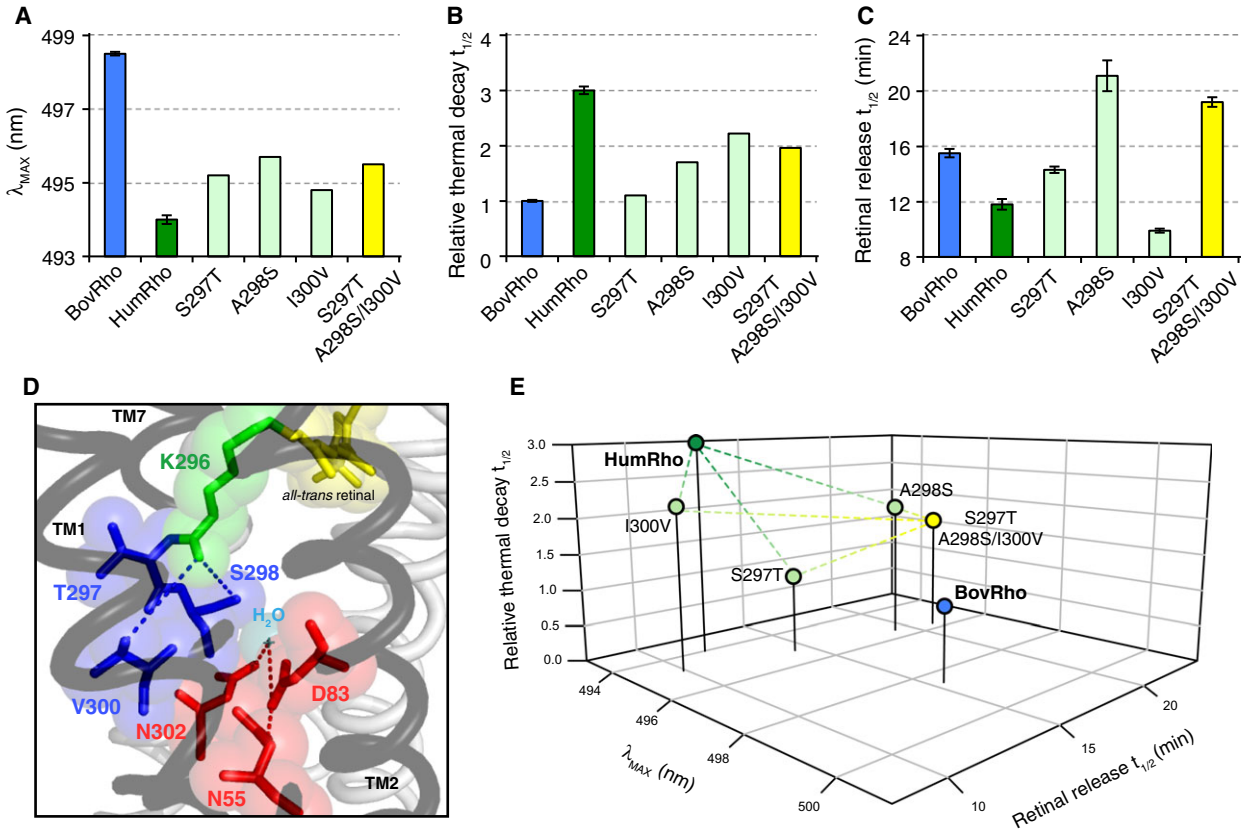

Fig. 2. Effects of substitutions near the Schiff base linkage on human rhodopsin function. The effects of mutations S297T, A298S, and I300V, along with a triple mutation, on (A) λ_{MAX}, (B) thermal decay, and (C) light-activated retinal release. (D) Crystal structure of bovine meta II (PDB code: 3PQR), highlighting the proximity of these sites to the Schiff base linkage with retinal. (E) 3D plot visualizing the contributions of these substitutions to the three functional properties investigated.

Table 2. Summary of functional data collected from wild-type and mutant rhodopsins.

Visual pigment	Mutation	λ_{MAX} (nm)[a]	Relative thermal decay half-life (min)[a]	Light-activated retinal release half-life (min)[a]
Bovine rhodospin	Wt	498.5 ± 0.05 (11)	1.00 ± 0.02 (9)	15.5 ± 0.30 (16)
Human rhodopsin	Wt	494.0 ± 0.12 (3)	3.00 ± 0.07 (2)	11.8 ± 0.38 (8)
	T213I	495.4	2.98	13.2 ± 0.35 (2)
	M216L	494.7	2.47	15.2 ± 0.30 (2)
	V266L	493.6	1.65	17.9 ± 0.55 (2)
	S270G	494.4	1.77	12.5 ± 0.10 (2)
	T213I/M216L/V266L/S270G	495.9	0.81	19.2 ± 0.52 (3)
	S297T	495.2	1.10	14.3 ± 0.23 (3)
	A298S	495.7	1.70	21.1 ± 1.11 (3)
	I300V	494.8	2.22	9.9 ± 0.15 (2)
	S297T/A298S/I300V	495.5	1.96	19.2 ± 0.35 (2)
Mammalia rhodopsin	Wt	—	1.66	—

[a] Values reported as mean ± standard error and number of replicates in parentheses when applicable.

Successive substitutions in TM5 and TM6 have an additive effect on kinetic functions

Bovine rhodopsin identities were also introduced at each of four nearby sites in human rhodopsin (T213I, M216L, V266L, S270G) located in TMs 5 and 6 to determine if any or all contributed to the functional discrepancies between human and bovine rhodopsin. Of the four single mutants, only T213I caused a red-shift in λ_{MAX} of more than 1 nm (495.4 nm), with M216L (494.7 nm), V266L (493.6 nm), and S270G (494.4 nm) resulting in very minor changes within the range of experimental variation (Fig. 3A). Meanwhile, the relative thermal decay half-life was shifted by some mutations towards a bovine rhodopsin phenotype, such as V266L (1.65) and S270G (1.77), whereas M216L (2.47) caused a more moderate change and T213I (2.98) did not vary from wild-type human rhodopsin (Fig. 3B). For the half-life of retinal release, V266L (17.9 ± 0.55 min) shifted to a rate longer than that of bovine rhodopsin, similar to the effect seen by the A298S mutation, although not as severe. The half-life of M216L (15.2 ± 0.30 min) was comparable to that of bovine rhodopsin, while both T213I (13.2 ± 0.35 min) and S270G (12.5 ± 0.10 min) caused smaller half-life increases (Fig. 3C). The fact that these substitutions contribute to kinetic properties related to the release of retinal may be due to their proximity to the hypothesized site of retinal release ([39,40]; Fig. 3D). Additionally, when all four mutations were combined, larger shifts in λ_{MAX} and kinetic rates were observed than for any single mutation, suggesting that a synergistic effect is occurring as substitutions accumulate around this structural motif that is influencing rhodopsin kinetics (Fig. 3E; Table 2).

The effect of retinitis pigmentosa mutation G51A depends on background sequence

We engineered and expressed G51A in a human rhodopsin background, alongside bovine rhodopsin, to determine if the effects of this RP mutation on *in vitro*

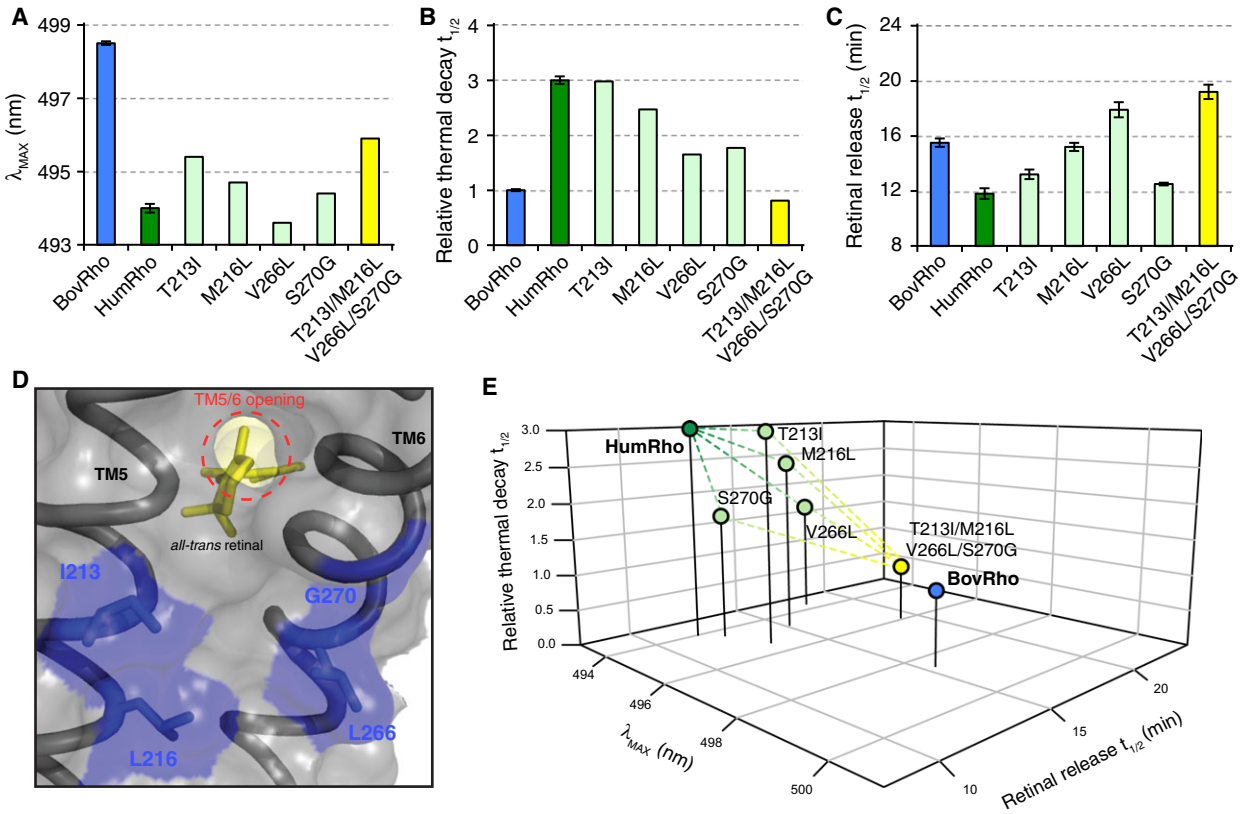

Fig. 3. Effects of substitutions near an opening between TMs 5 and 6 in light-activated rhodopsin. The effects of mutations T213I, M216L, V266L, S270G, along with a quadruple mutation, on (A) λ_{MAX}, (B) thermal decay, and (C) light-activated retinal release. (D) Crystal structure of bovine meta II (PDB code: 3PQR), highlighting the locations of these sites relative to the opening formed between TMs 5 and 6 during rhodopsin activation. (E) 3D plot visualizing the contributions of these substitutions to the three functional properties investigated.

rhodopsin function were uniform between the two mammalian pigments. When introduced into bovine rhodopsin, the G51A mutation led to a significantly longer retinal release half-life relative to wild-type (27.5 ± 2.44 min; +12.1 min vs. wild-type; Fig. 4A), which is comparable to previous studies [41,42]. Interestingly, when the same G51A substitution was made in human rhodopsin, the increase observed in the retinal release half-life (18.1 ± 1.81 min; +6.3 min vs. wild-type; Fig. 4B) was noticeably smaller than the difference in bovine rhodopsin (Fig. 4C). We supported this pattern statistically using a two-way analysis of variance (ANOVA), which showed a significant interaction effect between site 51 and species ($F_{1,24}$ = 27.7, P = 0.00002) that explained 17% of the variance in the data (Table 3). The majority of the variance (51%) was explained by the main effect from site 51 ($F_{1,24}$ = 81.4, P < 0.0001), but there was also a smaller contribution (13%) from the species main effect ($F_{1,24}$ = 22.4, P = 0.00008). This suggests that background sequence can influence the magnitude of functional change observed when introducing G51A, likely due to variable identities of nearby sites (Fig. 4D).

Human rhodopsin is more thermally stable than ancestral Mammalia rhodopsin

We expressed a previously reconstructed ancestral Mammalia rhodopsin [26] and measured thermal decay in order to better understand the evolutionary trajectories of human and bovine rhodopsin function. Mammalia rhodopsin consists of 355 amino acids, sharing 94.9% sequence identity with human rhodopsin (18 differences) and 92.4% sequence identity with bovine rhodopsin (27 differences). Additionally, Mammalia rhodopsin has human rhodopsin identities at six of the seven sites investigated in this study, with the only exception being S298, which follows the trend of terrestrial mammalian rhodopsins that seem more likely to have human rhodopsin identities at these sites (Fig. 5A). Interestingly, the relative thermal decay half-life of Mammalia rhodopsin (1.66) was longer than bovine rhodopsin, but shorter than human rhodopsin, suggesting that human rhodopsin is more thermally stable than even Mammalia rhodopsin (Fig. 5B). Both the λ_{MAX} (501.3 nm) and retinal release half-life (22.7 ± 0.66 min) of Mammalia rhodopsin have previously been measured [26]. Consequently, Mammalia rhodopsin differs from both bovine and human rhodopsin in all three functional properties reported in this study (Fig. 5C).

Discussion

Bovine rhodopsin is the prototypical visual pigment and has served as a model system for the vast majority of studies of rhodopsin structure and function, which includes the resolution of crystal structures of both dark [43,44] and activated states [45–47]. However, emerging evidence highlights the importance of comparative studies to address the variation in rhodopsin function [4,19,48], even among mammals [3,20]. This

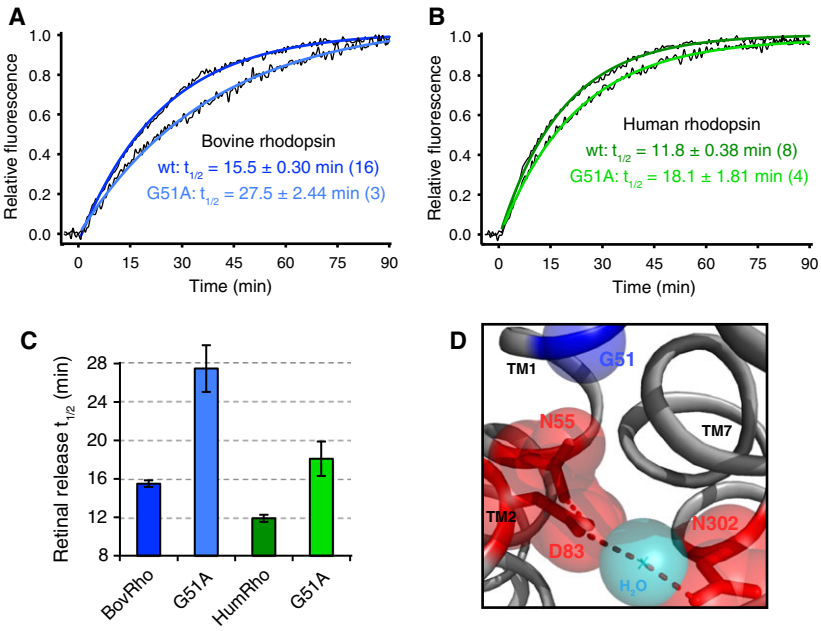

Fig. 4. RP-associated mutation G51A influences light-activated properties of bovine and human rhodopsin. (A–C) The G51A mutation causes a larger change to the half-life of light-activated retinal release in bovine rhodopsin compared to human rhodopsin, as measured by increased fluorescence following photoactivation. (D) Crystal structure of bovine meta II (PDB code: 3PQR) highlighting the proximity of site 51 to the N55-D83-N302 hydrogen-bonding network.

Table 3. Two-way ANOVA for the effect of species and site 51 on light-activated retinal release half-life.

Source of variation	*s.s.*	*d.f*	*m.s.*	*F*	*P*	*F* crit.	Omega sqr.
Factor #1 (Species)	95.57	1	95.57	22.44	0.00008	4.26	0.1370
Factor #2 (Site 51)	346.48	1	346.48	81.37	3.538E-9	4.26	0.5134
Interaction (Species × Site 51)	118.02	1	118.02	27.71	0.00002	4.26	0.1707
Error	102.20	24	4.26				
Total	662.27	27	24.53				
Effect size (Omega-squared)	0.8211						

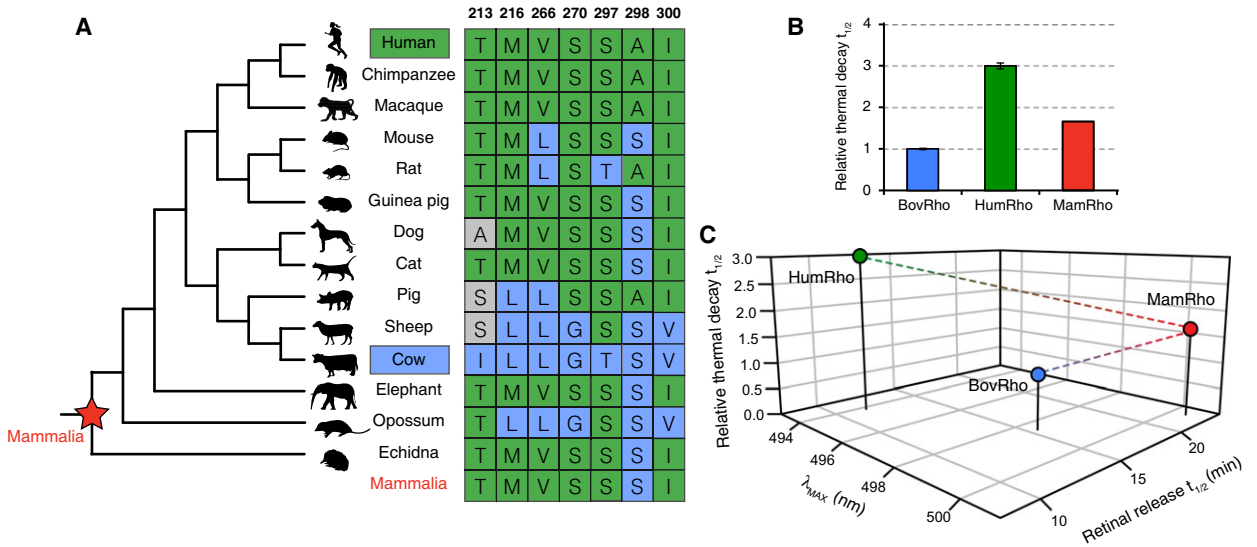

Fig. 5. Mammalia rhodopsin differs from bovine and human rhodopsin in all three functional properties investigated. (A) Schematic of the phylogenetic relationship of representatives of major terrestrial mammalian lineages, along with identities of rhodopsin amino acids at sites examined in this study. (B) Relative thermal decay rates of bovine, human, and Mammalia rhodopsin. (C) 3D plot visualizing a functional comparison of bovine, human, and Mammalia rhodopsin, including some previously published data [26].

trend also extends to human rhodopsin, where despite 93.4% sequence identity between the two pigments [28], several aspects of function differ from bovine rhodopsin, such as λ_{MAX} [23,24], and kinetics of rhodopsin intermediates following light activation [21,25]. This study shows that human rhodopsin and bovine rhodopsin also have significantly different rates of thermal decay and light-activated retinal release. While the larger discrepancy in rates of thermal decay is a surprising result, it follows a model that suggests an association between λ_{MAX} and thermal stability, where blue-shifted visual pigments are less susceptible to spontaneous thermal activation [49,50]. This effect may be based on differences in energy surfaces of the ground-state chromophore caused by amino acid substitutions between bovine and human rhodopsin [51]. It should also be noted that our experiments were performed in micelles of dodecyl maltoside, and that functional properties of visual pigments may vary when solubilized in different concentration or type of detergent [52,53], or when housed in lipid bicelles [54].

Our mutagenesis results localized two key motifs of rhodopsin structure that contribute to these functional discrepancies: (a) a trio of sites located within a single helical turn of the Schiff base linkage [2]; and (b) four sites near an opening between TM5 and TM6 that forms due to helical rearrangements during activation [39,40]. The most notable site investigated is 298, which mediates significant shifts in λ_{MAX}, thermal decay, and light-activated retinal release. This is likely explained by the proximity of site 298 to the K296 Schiff base linkage of the chromophore, and is consistent with the predicted effects of A298S on the electrostatic environment of the chromophore-binding pocket of human rhodopsin [21]. Mutations at nearby sites 297 and 300 also led to shifts in thermal decay and light-activated retinal release. These sites are also proximal to the N55-D83-N302 hydrogen bond chain that

places stabilizing interhelical constraints on TMs 1, 2, and 7 [55,56], and has been found to modulate differences in the kinetic properties of rhodopsin light-activation across different species [18]. Four other variable sites that were mutated (sites 213, 216, 266, 270) are positioned within 8 Å of the β-ionone ring of the chromophore in dark state rhodopsin and are part of TMs 5 and 6, the latter of which experiences an outward tilt during activation [57,58]. This results in an opening between TM5 and TM6 in the activated meta II state, which is thought to be the site where all-*trans*-retinal is released from opsin [39,40]. While individual substitutions at each of these sites only lead to modest changes in function, combining all four mutations led to much larger shifts in thermal decay and light-activated retinal release, which is concordant with previous studies that suggest variation at this motif can tune rhodopsin kinetics and that multiple mutations can lead to a more significant, additive effect [19,59].

Bovine rhodopsin has been a focus of studies investigating the molecular basis of hereditary retinal degeneration in humans, such as RP [60,61]. Despite advances in clinical diagnoses and treatments, the molecular characterization of RP remains a challenge due to the wide range of disease-associated mutations that yield variable molecular and clinical phenotypes [62,63]. These challenges emphasize the importance of reliable *in vitro* results that accurately reflect the impact of point mutations on protein function. The rhodopsin mutation G51A was first reported in the early 1990s following a screen of almost 300 subjects with RP [64]. Unlike some RP mutations that cannot be expressed *in vitro* due to severe misfolding or an inability to bind chromophore, G51A has been introduced into bovine rhodopsin, expressed, and functionally characterized [41]. Additionally, site 51 is thought to be involved in hydrogen-bonding interactions with N55 [65], with G51A resulting in altered stability of the dark and activated states of rhodopsin [42]. Our initial comparison suggests that variable sites 297, 298, and 300, which are proximal to the N55-D83-N302 hydrogen bond chain, help to mediate the functional differences between bovine and human rhodopsin and, therefore, may also influence the mutant phenotype of G51A that is associated with RP. Our results verify this hypothesis by showing that the effect of G51A on light-activated retinal release in human rhodopsin is different than that in bovine rhodopsin, with part of the contribution to the shift in function being due to background protein sequence. Moreover, this may imply that other RP-associated rhodopsin mutations proximal to the N55-D83-N302 hydrogen bond chain or the opening that forms in meta II between TMs 5 and 6 may cause altered effects to molecular function in human rhodopsin compared to bovine rhodopsin. Elucidating the variable impact in different protein backgrounds is critical for accurate understanding of the molecular basis of disease.

Examining rhodopsin through a comparative lens has been instrumental for enhancing our understanding of its function. For instance, highly conserved sites across mammalian rhodopsins have been shown to be more likely connected with disease-associated mutations [66]. Comparative sequence data were also used to infer the sequence of the ancestral mammalian rhodopsin pigment and resurrect the protein used in this study [60,61]. Ancestral mammals also have characteristics that suggest adaptations to a nocturnal lifestyle [67,68] that have traditionally been highlighted by evaluations of physiology [69] and fossil phenotypes [70] and are central to the specialized role of rhodopsin as a dim-light photoreceptor. However, more recent studies have reconstructed ancestral mammalian rhodopsin sequences using phylogenetic methods and performed expression and mutagenesis studies to evaluate the importance of specific residues to dim-light visual pigment function [26,71]. Here, we further characterize the mammalian rhodopsin protein reconstructed and expressed in our previous study [26] by determining that the dark state has a thermal decay half-life that is approximately intermediate between the half-life values of bovine and human rhodopsin. This is a curious result, considering that both the λ_{MAX} values and light-activated retinal release rates of bovine and human rhodopsin evolved in the same direction relative to ancestral Mammalia rhodopsin, but in opposing directions for thermal decay rates.

This study highlights important differences between the function of bovine and human rhodopsin, along with hypotheses relating to the major structural elements that may be involved in these differences. We continue to build on recent work aiming to better characterize human rhodopsin [21,25], most notably how it differs from bovine rhodopsin. This is particularly critical given mounting evidence for significant functional variation among mammalian rhodopsins [3,20,72]. Moreover, additional characterization of differences between bovine and human rhodopsin function will lend further insight into the mechanisms by which rhodopsin mutations may result in retinal disease.

Acknowledgements

We acknowledge Alex Van Nynatten for help with figure design and Dr. Rosalie Crouch for generously providing 11-*cis*-retinal. This work was supported by a Natural

Sciences and Engineering Research Council of Canada Discovery Grant (BSWC), a Foundation Fighting Blindness Seed Grant (BSWC), and Vision Science Research Program Scholarships (GMC, FEH, NB, SZD).

Author contributions

JMM and BSWC designed the research. JMM, GMC, SZD, PLT, and NB performed the research. JMM and GMC wrote the paper, with contributions from SZD and FEH, and guidance and edits from BSWC. BSWC supervised all aspects of the study.

References

1 Burns ME and Baylor DA (2001) Activation, deactivation, and adaptation in vertebrate photoreceptor cells. *Annu Rev Neurosci* **24**, 779–805.
2 Sakmar TP, Franke RR and Khorana HG (1989) Glutamic acid-113 serves as the retinylidene Schiff base counterion in bovine rhodopsin. *Proc Natl Acad Sci USA* **86**, 8309–8313.
3 Dungan SZ, Kosyakov A and Chang BS (2016) Spectral tuning of killer whale (*Orcinus orca*) rhodopsin: evidence for positive selection and functional adaptation in a cetacean visual pigment. *Mol Biol Evol* **33**, 323–336.
4 Schott RK, Müller J, Yang CG, Bhattacharyya N, Chan N, Xu M, Morrow JM, Ghenu AH, Loew ER, Tropepe V *et al.* (2016) Evolutionary transformation of rod photoreceptors in the all-cone retina of a diurnal garter snake. *Proc Natl Acad Sci USA* **113**, 356–361.
5 Baylor D (1996) How photons start vision. *Proc Natl Acad Sci USA* **93**, 560–565.
6 Baylor DA, Matthews G and Yau KW (1980) Two components of electrical dark noise in toad retinal rod outer segments. *J Physiol* **309**, 591–621.
7 Hofmann KP, Pulvermuller A, Buczylko J, Van Hooser P and Palczewski K (1992) The role of arrestin and retinoids in the regeneration pathway of rhodopsin. *J Biol Chem* **267**, 15701–15706.
8 Hartong DT, Berson EL and Dryja TP (2006) Retinitis pigmentosa. *Lancet* **368**, 1795–1809.
9 Fuchs S, Kranich H, Denton MJ, Zrenner E, Bhattacharya SS, Humphries P and Gal A (1994) Three novel rhodopsin mutations (C110F, L131P, A164V) in patients with autosomal dominant retinitis pigmentosa. *Hum Mol Genet* **3**, 1203.
10 Olsson JE, Gordon JW, Pawlyk BS, Roof D, Hayes A, Molday RS, Mukai S, Cowley GS, Berson EL and Dryja TP (1992) Transgenic mice with a rhodopsin mutation (Pro23His): a mouse model of autosomal dominant retinitis pigmentosa. *Neuron* **9**, 815–830.
11 Macke JP, Hennessey JC and Nathans J (1995) Rhodopsin mutation proline347-to-alanine in a family with autosomal dominant retinitis pigmentosa indicates an important role for proline at position 347. *Hum Mol Genet* **4**, 775–776.
12 Tsui I, Chou CL, Palmer N, Lin CS and Tsang SH (2008) Phenotype-genotype correlations in autosomal dominant retinitis pigmentosa caused by RHO, D190N. *Curr Eye Res* **33**, 1014–1022.
13 Stojanovic A, Hwang I, Khorana HG and Hwa J (2003) Retinitis pigmentosa rhodopsin mutations L125R and A164V perturb critical interhelical interactions: new insights through compensatory mutations and crystal structure analysis. *J Biol Chem* **278**, 39020–39028.
14 Liu MY, Liu J, Mehrotra D, Liu Y, Guo Y, Baldera-Aquayo PA, Mooney VL, Nour AM and Yan EC (2013) Thermal stability of rhodopsin and progression of retinitis pigmentosa: comparison of S186W and D190N rhodopsin mutants. *J Biol Chem* **288**, 17698–17712.
15 Opefi CA, South K, Reynolds CA, Smith SO and Reeves PJ (2013) Retinitis pigmentosa mutants provide insight into the role of the N-terminal cap in rhodopsin folding, structure, and function. *J Biol Chem* **288**, 33912–33926.
16 Mendes HF, van der Spuy J, Chapple JP and Cheetham ME (2005) Mechanisms of cell death in rhodopsin retinitis pigmentosa: implications for therapy. *Trends Mol Med* **11**, 177–185.
17 Papermaster DS (1982) Preparation of retinal rod outer segments. *Methods Enzymol* **81**, 48–52.
18 Sugawara T, Imai H, Nikaido M, Imamoto Y and Okada N (2010) Vertebrate rhodopsin adaptation to dim light via rapid meta-II intermediate formation. *Mol Biol Evol* **27**, 506–519.
19 Morrow JM and Chang BS (2015) Comparative mutagenesis studies of retinal release in light-activated zebrafish rhodopsin using fluorescence spectroscopy. *Biochemistry* **54**, 4507–4518.
20 Bickelmann C, Morrow JM, Müller J and Chang BS (2012) Functional characterization of the rod visual pigment of the echidna (*Tachyglossus aculeatus*), a basal mammal. *Vis Neurosci* **29**, 211–217.
21 Kazmin R, Rose A, Szczepek M, Elgeti M, Ritter E, Piechnick R, Hofmann KP, Scheerer P, Hildebrand PW and Bartl FJ (2015) The activation pathway of human rhodopsin in comparison to bovine rhodopsin. *J Biol Chem* **290**, 20117–20127.
22 Rakoczy EP, Kiel C, McKeone R, Stricher F and Serrano L (2011) Analysis of disease-linked rhodopsin mutations based on structure, function, and protein stability calculations. *J Mol Biol* **405**, 584–606.
23 Wald G, Brown PK and Smith PH (1955) Iodopsin. *J Gen Physiol* **38**, 623–681.
24 Oprian DD, Molday RS, Kaufman RJ and Khorana HG (1987) Expression of a synthetic bovine rhodopsin

gene in monkey kidney cells. *Proc Natl Acad Sci USA* **84**, 8874–8878.
25 Funatogawa C, Szundi I and Kliger DS (2016) A comparison between the photoactivation kinetics of human and bovine rhodopsins. *Biochemistry* **55**, 7005–7013.
26 Bickelmann C, Morrow JM, Du J, Schott RK, van Hazel I, Lim S, Müller J and Chang BS (2015) The molecular origin and evolution of dim-light vision in mammals. *Evolution* **69**, 2995–3003.
27 Ferretti L, Karnik SS, Khorana HG, Nassal M and Oprian DD (1986) Total synthesis of a gene for bovine rhodopsin. *Proc Natl Acad Sci USA* **83**, 599–603.
28 Nathans J and Hogness DS (1984) Isolation and nucleotide sequence of the gene encoding human rhodopsin. *Proc Natl Acad Sci USA* **81**, 4851–4855.
29 Morrow JM and Chang BS (2010) The p1D4-hrGFP II expression vector: a tool for expressing and purifying visual pigments and other G protein-coupled receptors. *Plasmid* **64**, 162–169.
30 Molday RS and MacKenzie D (1983) Monoclonal antibodies to rhodopsin: characterization, cross-reactivity, and application as structural probes. *Biochemistry* **22**, 653–660.
31 Govardovskii VI, Fyhrquist N, Reuter T, Kuzmin DG and Donner K (2000) In search of the visual pigment template. *Vis Neurosci* **17**, 509–528.
32 Farrens DL and Khorana HG (1995) Structure and function in rhodopsin. Measurement of the rate of metarhodopsin II decay by fluorescence spectroscopy. *J Biol Chem* **270**, 5073–5076.
33 Fujikoshi Y (1993) Two-way ANOVA models with unbalanced data. *Discrete Math* **116**, 315–334.
34 Dungan SZ and Chang BS (2017) Epistatic interactions influence terrestrial-marine functional shifts in cetacean rhodopsin. *Proc Biol Sci* **284**, 20162743.
35 Tukey JW (1949) Comparing individual means in the analysis of variance. *Biometrics* **5**, 99–114.
36 Guo Y, Sekharan S, Liu J, Batista VS, Tully JC and Yan EC (2014) Unusual kinetics of thermal decay of dim-light photoreceptors in vertebrate vision. *Proc Natl Acad Sci USA* **111**,10438–10443.
37 Yan EC, Kazmi MA, De S, Chang BS, Seibert C, Marin EP, Mathies RA and Sakmar TP (2002) Function of extracellular loop 2 in rhodopsin: glutamic acid 181 modulates stability and absorption wavelength of metarhodopsin II. *Biochemistry* **41**, 3620–3627.
38 Chen MH, Kuemmel C, Birge RR and Knox BE (2012) Rapid release of retinal from a cone visual pigment following photoactivation. *Biochemistry* **51**, 4117–4125.
39 Schädel SA, Heck M, Maretzki D, Filipek S, Teller DC, Palczewski K and Hofmann KP (2003) Ligand channeling within a G-protein-coupled receptor. The entry and exit of retinals in native opsin. *J Biol Chem* **278**, 24896–24903.
40 Hildebrand PW, Scheerer P, Park JH, Choe HW, Piechnick R, Ernst OP, Hofmann KP and Heck M (2009) A ligand channel through the G protein coupled receptor opsin. *PLoS ONE* **4**, e4382.
41 Hwa J, Garriga P, Liu X and Khorana HG (1997) Structure and function in rhodopsin: packing of the helices in the transmembrane domain and folding to a tertiary structure in the intradiscal domain are coupled. *Proc Natl Acad Sci USA* **94**, 10571–10576.
42 Bosch L, Ramon E, Del Valle LJ and Garriga P (2003) Structural and functional role of helices I and II in rhodopsin. A novel interplay evidenced by mutations at Gly-51 and Gly-89 in the transmembrane domain. *J Biol Chem* **278**, 20203–20209.
43 Palczewski K, Kumasaka T, Hori T, Behnke CA, Motoshima H, Fox BA, Le Trong I, Teller DC, Okada T, Stenkamp RE *et al*. (2000) Crystal structure of rhodopsin: a G protein-coupled receptor. *Science* **289**, 739–745.
44 Okada T, Sugihara M, Bondar AN, Elstner M, Entel P and Buss V (2004) The retinal conformation and its environment in rhodopsin in light of a new 2.2 A crystal structure. *J Mol Biol* **342**, 571–583.
45 Park JH, Scheerer P, Hofmann KP, Choe HW and Ernst OP (2008) Crystal structure of the ligand-free G-protein-coupled receptor opsin. *Nature* **454**, 183–187.
46 Scheerer P, Park JH, Hildebrand PW, Kim YJ, Krauss N, Choe HW, Hofmann KP and Ernst OP (2008) Crystal structure of opsin in its G-protein-interacting conformation. *Nature* **455**, 497–502.
47 Choe HW, Kim YJ, Park JH, Morizumi T, Pai EF, Krauss N, Hofmann KP, Scheerer P and Ernst OP (2011) Crystal structure of metarhodopsin II. *Nature* **471**, 651–655.
48 van Hazel I, Dungan SZ, Hauser FE, Morrow JM, Endler JA and Chang BS (2016) A comparative study of rhodopsin function in the great bowerbird (*Ptilonorhynchus nuchalis*): spectral tuning and light-activated kinetics. *Protein Sci* **25**, 1308–1318.
49 Gozem S, Schapiro I, Ferre N and Olivucci M (2012) The molecular mechanism of thermal noise in rod photoreceptors. *Science* **337**, 1225–1228.
50 Luk HL, Bhattacharyya N, Montisci F, Morrow JM, Melaccio F, Wada A, Sheves M, Fanelli F, Chang BS and Olivucci M (2016) Modulation of thermal noise and spectral sensitivity in Lake Baikal cottoid fish rhodopsins. *Sci Rep* **6**, 38425.
51 Gozem S, Huntress M, Schapiro I, Lindh R, Granovsky AA, Angeli C and Olivucci M (2012) Dynamic electron correlation effects on the ground state potential energy surface of a retinal chromophore model. *J Chem Theory Comput* **8**, 4069–4080.

52 König B, Welte W and Hofmann KP (1989) Photoactivation of rhodopsin and interaction with transducin in detergent micelles. Effect of 'doping' with steroid molecules. *FEBS Lett* **257**, 163–166.
53 Ramon E, Marron J, del Valle L, Bosch L, Andrés A, Manyosa J and Garriga P (2003) Effect of dodecyl maltoside detergent on rhodopsin stability and function. *Vision Res* **43**, 3055–3061.
54 McKibbin C, Farmer NA, Jeans C, Reeves PJ, Khorana HG, Wallace BA, Edwards PC, Villa C and Booth PJ (2007) Opsin stability and folding: modulation by phospholipid bicelles. *J Mol Biol* **374**, 1319–1332.
55 Rath P, DeCaluwe LL, Bovee-Geurts PH, DeGrip WJ and Rothschild KJ (1993) Fourier transform infrared difference spectroscopy of rhodopsin mutants: light activation of rhodopsin causes hydrogen-bonding change in residue aspartic acid-83 during meta II formation. *Biochemistry* **32**, 10277–10282.
56 Breikers G, Bovee-Geurts PH, DeCaluwe GL and DeGrip WJ (2001) A structural role for Asp83 in the photoactivation of rhodopsin. *Biol Chem* **382**, 1263–1270.
57 Farrens DL, Altenbach C, Yang K, Hubbell WL and Khorana HG (1996) Requirement of rigid-body motion of transmembrane helices for light activation of rhodopsin. *Science* **274**, 768–770.
58 Eilers M, Goncalves JA, Ahuja S, Kirkup C, Hirshfeld A, Simmerling C, Reeves PJ, Sheves M and Smith SO (2012) Structural transitions of transmembrane helix 6 in the formation of metarhodopsin I. *J Phys Chem B* **116**, 10477–10489.
59 Piechnick R, Ritter E, Hildebrand PW, Ernst OP, Scheerer P, Hofmann KP and Heck M (2012) Effect of channel mutations on the uptake and release of the retinal ligand in opsin. *Proc Natl Acad Sci USA* **109**, 5247–5252.
60 Garriga P, Liu X and Khorana HG (1996) Structure and function in rhodopsin: correct folding and misfolding in point mutants at and in proximity to the site of the retinitis pigmentosa mutation Leu-125--> Arg in the transmembrane helix C. *Proc Natl Acad Sci USA* **93**, 4560–4564.
61 Ramon E, Cordomi A, Aguila M, Srinivasan S, Dong X, Moore AT, Webster AR, Cheetham ME and Garriga P (2014) Differential light-induced responses in sectorial inherited retinal degeneration. *J Biol Chem* **289**, 35918–35928.
62 Anasagasti A, Irigoyen C, Barandika O, López de Munain A and Ruiz-Ederra J (2012) Current mutation discovery approaches in Retinitis Pigmentosa. *Vision Res* **75**, 117–129.
63 McKeone R, Wikstrom M, Kiel C and Rakoczy PE (2014) Assessing the correlation between mutant rhodopsin stability and the severity of retinitis pigmentosa. *Mol Vis* **20**, 183–199.
64 Macke JP, Davenport CM, Jacobson SG, Hennessey JC, Gonzalez-Fernandez F, Conway BP, Heckenlively J, Palmer R, Maumenee IH, Sieving P *et al.* (1993) Identification of novel rhodopsin mutations responsible for retinitis pigmentosa: implications for the structure and function of rhodopsin. *Am J Hum Genet* **53**, 80–89.
65 Smith SO (2010) Structure and activation of the visual pigment rhodopsin. *Annu Rev Biophys* **39**, 309–328.
66 Hauser FE, Schott RK, Castiglione GM, Van Nynatten A, Kosyakov A, Tang PL, Gow DA and Chang BS (2016) Comparative sequence analyses of rhodopsin and RPE65 reveal patterns of selective constraint across hereditary retinal disease mutations. *Vis Neurosci* **33**, 1–13.67.
67 Crompton AW, Taylor CR and Jagger JA (1978) Evolution of homeothermy in mammals. *Nature* **272**, 333–336.
68 Luo ZX, Chen P, Li G and Chen M (2007) A new eutriconodont mammal and evolutionary development in early mammals. *Nature* **446**, 288–293.
69 Hall MI, Kamilar JM and Kirk EC (2012) Eye shape and the nocturnal bottleneck of mammals. *Proc Biol Sci* **279**, 4962–4968.
70 Angielczyk KD and Schmitz L (2014) Nocturnality in synapsids predates the origin of mammals by over 100 million years. *Proc Biol Sci* **281**, 20141642.
71 Fernandez-Sampedro MA, Invergo BM, Ramon E, Bertranpetit J and Garriga P (2016) Functional role of positively selected amino acid substitutions in mammalian rhodopsin evolution. *Sci Rep* **6**, 21570.
72 Hunt DM, Arrese CA, von Dornum M, Rodger J, Oddy A, Cowing JA, Ager EI, Bowmaker JK, Beazley LD and Shand J (2003) The rod opsin pigments from two marsupial species, the South American bare-tailed woolly opossum and the Australian fat-tailed dunnart. *Gene* **323**, 157–162.